NANO LETTERS

Letter

pubs.acs.org/NanoLett

Diffusive versus Displacive Contact Plasticity of Nanoscale Asperities: Temperature- and Velocity-Dependent Strongest Size

Wei Guo,[†] Zhao Wang,*[,†] and Ju Li*[,‡]

[†]Frontier Institute of Science and Technology, and State Key Laboratory for Mechanical Behavior of Materials, Xi'an Jiaotong University, 710054, Xi'an, People's Republic of China

[‡]Department of Nuclear Science and Engineering and Department of Materials Science and Engineering, Massachusetts Institute of Technology, Cambridge, Massachusetts 02139, United States

Supporting Information

ABSTRACT: We predict a strongest size for the contact strength when asperity radii of curvature decrease below 10 nm. The reason for such strongest size is found to be correlated with the competition between the dislocation plasticity and surface diffusional plasticity. The essential role of temperature is calculated and illustrated in a comprehensive asperity size-strength-temperature map taking into account the effect of contact velocity. Such a map should be essential for various phenomena related to nanoscale contacts such as nanowire cold welding, self-assembly of nanoparticles and adhesive nanopillar arrays, as well as the electrical, thermal, and mechanical properties of macroscopic interfaces.

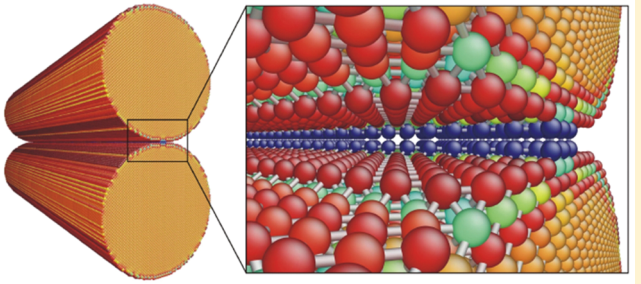

Nanoscale contact between two curved surfaces

KEYWORDS: *Material strength, dislocation plasticity, surface diffusion, sub-10 nm, Zener-Hollomon scaling*

When two macroscopic solids touch, the atomistic realities of their nanoscale contacts are hidden from easy view, but they actually control how heat, electrical charge, and forces are transferred across the rough interface.[1] The true contact area, A_{true}, defined by atoms of the two bodies that truly interact atomistically (within certain interatomic force/distance cutoffs), is usually much smaller than the nominal macroscopic contact area A. A_{true}/A usually decreases with increasing surface roughness of the two bodies and increases with externally applied pressure $P_{ext} \equiv -F_{ext}/A$. Recently, Pastewka and Robbins showed numerically using linear elasticity and half-space Green's function how A_{true}/A depends on P_{ext} (e.g., linearly) for two self-affine random surfaces, statistically self-similar within profile wavelengths $[\lambda_s, \lambda_L]$.[2] They found that when the solids are elastically compliant enough, the ratio between A_{true}/A and P_{ext} diverges due to microscopic adhesion, signifying a "non-sticky"-to-"sticky" transition of the macro-contact.

While Pastewka and Robbins' results are revealing, the assumptions of linear elasticity, especially at the lower wavelength cutoff λ_s "of order nanometers",[2] could be limiting. This is because plasticity by dislocation motion and/or diffusion can occur, certainly at high enough P_{ext}, but may also occur at $P_{ext} = 0$, as we show below. One may also ask what could be a physical basis for the λ_s cutoff in solving elasticity problems: is this assumed initial condition reflecting prior history with surface diffusional plasticity[3] that tends to smooth out profile roughnesses finer than λ_s? Incidentally, for nanostructures Jiang et al.[4] and Guisbiers and Buchaillot[5] have proposed size-dependent effective diffusivity

$$D(T, R) = D_{0\infty} \exp\left[-\frac{CT_{m\infty}}{k_B T}\left(1 - \frac{\tilde{\alpha}}{2R}\right)\right] \quad (1)$$

affecting nanoscale creep that accompanies the well-established melting-point reduction[6,7]

$$T_m(R) = T_{m\infty}\left(1 - \frac{\alpha}{2R}\right) \quad (2)$$

where R is the radius of curvature of the nanoasperity, $T_{m\infty}$ is the bulk thermodynamic melting point, k_B is the Boltzmann constant, and $C,\alpha,\tilde{\alpha},D_{0\infty}$ are temperature- and size-independent positive constants. Such "exponentially accelerated" small-size diffusive kinetics in eq 1 seem to have some experimental support.[8,9] While the physical basis for eq 1 is not as well-understood as eq 2, one notes that in the $R < 10$ nm, and lower-homologous-temperature deformation regime that we are mostly interested in, the effective diffusivity $D(T,R)$ is dominated by the surface diffusion contribution. The activation energy Q_S of surface diffusion mathematically could have a leading-order correction proportional to $1/R$ in an asymptotic expansion with respect to curvature that physically could be due to, for example, elasticity effect of the saddle-point config-

Received: June 10, 2015
Revised: August 8, 2015
Published: August 31, 2015

DOI: 10.1021/acs.nanolett.5b02306
Nano Lett. 2015, 15, 6582−6585

uration of diffusion, or the ratio of atoms near surface crystallographic facet−facet intersections ("surface defects") among all surface atoms. In other words, the curvature effect on surface diffusion may be explained by the curvature-dependent concentration and mobility of "surface defects". Surface diffusion could be the key for understanding λ_s. Recently, it was demonstrated experimentally that under an external load or a capillarity-generated Young−Laplace pressure, plasticity by surface diffusion can indeed happen at sub-10 nm length scale at room temperature.[10,11]

With the above motivation, it is critical to understand the characteristics of plasticity for nanoscale asperities. Many experiments have shown that individual nanostructures can sustain close to their ideal strength[12] due to dislocation starvation. The "smaller is stronger" trend provides a strategy for increasing the material strength by nanostructuring. However, when R goes down to even smaller, surface diffusion could cause dramatic softening and "smaller is much weaker".[13] Here we look into this issue of diffusive versus displacive contact plasticity by atomistic simulations using the classical molecular dynamics (MD) simulator LAMMPS.[14] As shown in the inset of Figure 1, in our simulations two identical metal

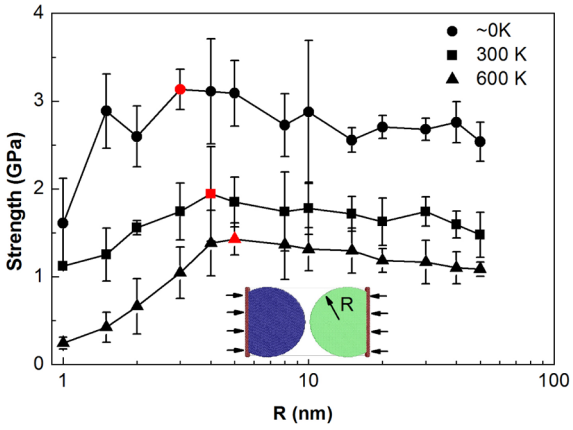

Figure 1. Contact strength as a function of the asperity radius R at different temperatures. The peak values corresponding to the strongest size are marked with red symbols. Error bars are based on the deviation of difference in three crystal orientations. Note that the strength is averaged over three crystal orientations ([100] against [100], [100] against [110], and [100] against [16 5 0]) with respect to the two face-centered-cubic crystals.

cylinders are moved toward each other. An embedded atom method potential[15] was used to describe the atomistic interaction of Al, which is chosen because of its elastic isotropy that simplifies the analysis. We have applied displacement control $-2\Delta x(t)$ between the two rigid outer boundaries in our simulations. To contrast the outcome of different-size nano-asperities, we define total strain as $\varepsilon \equiv \Delta x(t)/R$. The stress is defined by the engineering stress convention $\sigma_{\text{engineering}} \equiv F/A$, where F is the computed total force sustained in one of the rigid outer boundaries, and $A \equiv (2R)L$ is the initial projected cross-sectional area of the cylinder, which is a "nominal" contact area in this simulation. In this paper, the "strength" of contact is defined as the time-average of $\sigma_{\text{engineering}}$ in the strain range 0.08−0.2 during loading, so it should be interpreted as plastic "flow strength" and not the initiation or yield strength (see stress−strain curve in Supporting Information for explanation of the strength measure used). R is varied from 1 to 50 nm and the strain rate $\dot{\varepsilon}$ is about 10^8−10^9/s. MD simulations were performed using a Nosé−Hoover thermostat, and the systems were relaxed for 2 ps at each load step of 0.1 Å. We note that the strain rate range 10^8−10^9/s in our simulations does not induce significant difference in the final contact strengths reported.

The size-strength relationship of our cylindrical contacts at T = 0, 300, and 600 K are plotted in Figure 1. It clearly shows that there exists a strongest size for the contact strength, below which the "smaller is stronger" trend no longer holds. The sharp decrease in strength when the contact size goes down to sub-10 nm scale contradicts with the lattice dislocation-mediated deformation mechanism[16,17] and suggests that the strongest size is in a deformation mechanism transition zone. In our simulated samples, the critical sizes range from 5 to 10 nm. In this size range, the difference between crystal and liquid surface energies causes the crystal melting point T_m to decrease as described by eq 2, and this effect is particularly significant in the case of R < 10 nm.[7] Thus, it can be expected that the surface atom diffusion may become important for the strongest size, especially when the nanoasperity is under a high load.

We have performed detailed analyses of the atomistic configurations and stress distributions in the simulated samples, as shown in Figure 2. A classical Hertzian stress pattern is found

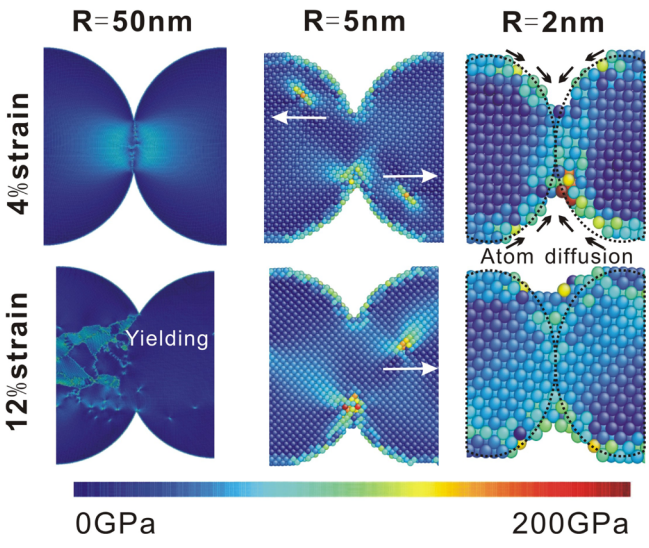

Figure 2. Snapshots of simulated room-temperature contacts of three different sizes at two different applied strain levels. The color of atoms represents the von Mises stress distribution. The arrows in the middle panel show the direction of dislocation displacement during loading. The arrows in the right panel show the direction of atomistic diffusion flow.

beneath the interface of the largest contact (R = 50 nm) at 4% strain, and the system starts to deform plastically before 12% strain. In a smaller contact (R = 5 nm), a pair of dislocations is found to form beneath the interface and move to interior following increasing compressive load. This dislocation activity results in a more homogeneous stress distribution in the contacting bodies. When R decreases further down to 2 nm, we visually found that the surface atoms diffuse significantly even at room temperature, which is in agreement with first-principles calculations.[18] The atoms inside remain highly crystalline while surface atoms diffuse to the neck region. Similar room-temperature "liquid-like" deformation behaviors were observed

DOI: 10.1021/acs.nanolett.5b02306
Nano Lett. 2015, 15, 6582−6585

in experiments on Ag nanoparticles of about 10 nm diameter,[10] as well as the cold welding of Au nanowires (3−10 nm diameter).[19]

To quantify diffusion in small samples under load, we apply the "deformation-diffusion" decomposition,[20−22]

$$D_i^2 = \frac{1}{N_i}\min_{\mathbf{J}_i}\sum_{j\in N_i}|\mathbf{d}_{ji}^0\mathbf{J}_i - \mathbf{d}_{ji}|^2 \tag{3}$$

where i,j index atoms, D_i^2 is a measure of magnitude of non-affine motion of atoms around i; $j\in N_i$ are i's initial neighbors at the reference configuration, $\mathbf{d}_{ji}^0$ is the distance vector between atom j and i at the reference configuration, and $\mathbf{d}_{ji}$ is the current distance vector. The local deformation gradient $\mathbf{J}_i$ is numerically optimized to minimize D_i^2. On the right-hand side, $\mathbf{d}_{ji}^0\mathbf{J}_i$ stands for the displacive deformation, while $\mathbf{d}_{ji}^0\mathbf{J}_i-\mathbf{d}_{ji}$ refers to the contribution of the non-affine, or diffusional part of the displacement.[20] When the contacting bodies are compressed to deformed plastically, we can see the mean D^2 fluctuates as that shown in Figure 3a due to the dislocation plasticity and

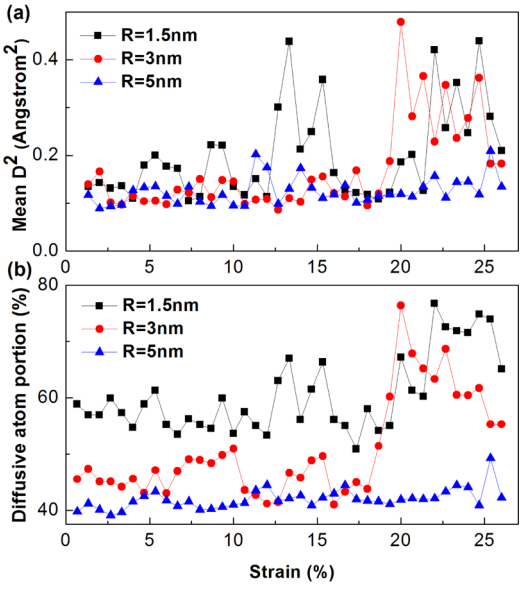

Figure 3. (a) Mean D^2 as a function of the strain in three contacts of different curvature radii. (b) Diffusive atom ratios as a function of the strain.

structure collapse. It is shown that D^2 for R = 1.5 nm contact is the largest indicating a clearly enhanced atom diffusion. We borrow the threshold value from Lindemann criterion,[23] which was used to predict the melting point of surface confined materials, to qualitatively compare the extent of diffusion during loading. For simplicity we label an atom as diffusive when its $\sqrt{D_i^2}$ exceeds the 10% of the nearest neighbor distance. Figure 3b shows that a smaller contact contains a higher ratio of diffusive atoms, an observation consistent with the nanowire and nanoparticle experiments.[5,23,24] In our R = 2 nm sample, the surface diffusion results in lower plastic flow stress and better adhesion. Even though the diffusion is clearly accelerated by the atomic random thermal motion when the temperature increases,[18] we can also observe stress-induced surface diffusion even at $T \to 0$ K (see our energy minimization simulation results in Supporting Information). It was suggested that this type of diffusion can be not only thermally activated but also driven by externally applied stress[22] and/or surface tension.[11,25]

The results above showed that the contact becomes "smaller is weaker" when the surface atom diffusion dominates. On the basis of our simulation data, we obtain a comprehensive contact size-strength-temperature map in Figure 4, illustrating the

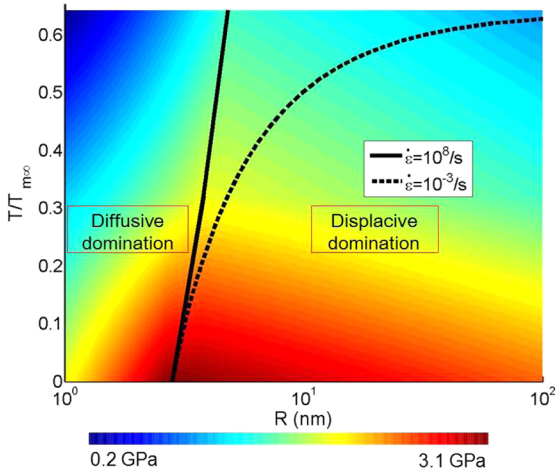

Figure 4. Contact strength mechanism map as a function of the radius of curvature (R) and homologous temperature ($T/T_{m\infty}$). The color range represents the strength values. The highest contact asperity strength computed with MD at $\dot{\varepsilon} = 10^8$/s is outlined by the solid curve. The dashed curve represents the strongest contact size under an ordinary experimental strain rate.

competition between the displacive and diffusion mechanisms. We find the strongest size R_c and homologous temperature $T/T_{m\infty}$ from simulations can be well-fitted as follows

$$R_c = A\frac{T}{T_{m\infty}} + B \tag{4}$$

We obtain A = 3.1 nm and B = 2.8 nm by fitting to our MD simulation data. However, this result should not be directly applicable to laboratory experiments since the strain rate of the MD simulations could be many orders of magnitude higher. To overcome this limitation, we use an empirical velocity-modified temperature approach[26] based on the Zener-Hollomon parameter that bridges the strain rate and the temperature. This approach considers that increasing the strain rate has the similar effect as decreasing the temperature upon the stress−strain relation.[27] This semiempirical relation bridges the temperature and strain rate as

$$T_{exp} = T_{MD}\left(1 - \frac{k_B T_{exp}}{Q_S}\ln\frac{\dot{\varepsilon}_{MD}}{\dot{\varepsilon}_{exp}}\right) \tag{5}$$

where Q_S is an activation energy, $\dot{\varepsilon}_{MD}$ is the simulation strain rate, T_{exp} is the experimental temperature, and $\dot{\varepsilon}_{exp}$ is the experimental strain rate. The Zener-Hollomon corrected strongest size can be derived when we combine eqs 4 and 5 to write

$$R_c = \frac{T_{exp}}{T_{m\infty}}\left(\frac{A}{1 - \frac{k_B T_{exp}}{Q_S}\ln\left(\frac{\dot{\varepsilon}_{MD}}{\dot{\varepsilon}_{exp}}\right)}\right) + B \tag{6}$$

DOI: 10.1021/acs.nanolett.5b02306
Nano Lett. 2015, 15, 6582−6585

We assume that $\dot{\varepsilon}_{exp} = 10^{-3}$/s as a typical laboratory experiment strain rate, and Q_S = 126 kJ/mol = 1.3 eV for the aluminum system studied here,[28] which should be an upper bound for processes controlled by surface diffusion (and therefore gives the most sensitive strain-rate dependence). The predicted temperature-size effects at $\dot{\varepsilon}_{exp} = 10^{-3}$/s is shown by the dashed curve in Figure 4. The sub-10 nm Au tips[29] and Ag particles[10] at homologous temperature $T_{exp}/T_{m\infty}$ of 0.22 and 0.24 are then in the diffusion-dominated regime, which are in agreement with previous experimental observations.[10,29]

Bridging the gap between nanoscale contacts and the electrical, thermal and mechanical properties of rough macroscopic interfaces[2,30−32] must require accurate information about the size-dependent plasticity. From Figure 1, it can be seen that the strength drops precipitously[13] when the asperity size goes below R_c. The plastic deformation strength, which was often considered a constant, is clearly a function of the asperity size. Moreover, the correlation between the critical size and temperature/strain rate provides some physical basis for λ_s, and also a criterion to judge whether the asperity in contact is in the diffusion-controlled regime (Figure 4), which if so is expected to bond more strongly. Such criterion may be applied to material cold welding[1,19] and self-assembly[33] and for physics-based modeling of the electrical, thermal, and mechanical properties of contacts.

■ ASSOCIATED CONTENT

Supporting Information

The Supporting Information is available free of charge on the ACS Publications website at DOI: 10.1021/acs.nanolett.5b02306.

Surface atom diffusion to contact region, crystal orientation dependence of the contact strength, and stress-strain curve for explaining the strength measure. (PDF)

■ AUTHOR INFORMATION

Corresponding Authors

*E-mail: wzzhao@yahoo.fr.
*E-mail: liju@mit.edu

Notes

The authors declare no competing financial interest.

■ ACKNOWLEDGMENTS

This work is supported by a grant-in-aid of 985 Project from Xi'an Jiaotong University, the National Natural Science Foundation of China (Grant 11204228) and the National Basic Research Program of China (2012CB619402 and 2014CB644003). J.L. acknowledges support by NSF DMR-1410636 and DMR-1120901.

■ REFERENCES

(1) Ferguson, G. S.; Chaudhury, M. K.; Sigal, G. B.; Whitesides, G. M. *Science* **1991**, *253*, 776.
(2) Pastewka, L.; Robbins, M. O. *Proc. Natl. Acad. Sci. U. S. A.* **2014**, *111*, 3298.
(3) Li, J. *Nat. Mater.* **2015**, *14*, 656.
(4) Jiang, Q.; Zhang, S.; Li, J. *Solid State Commun.* **2004**, *130*, 581.
(5) Guisbiers, G.; Buchaillot, L. *Nanotechnology* **2008**, *19*, 435701.
(6) Buffat, P.; Borel, J. P. *Phys. Rev. A: At., Mol., Opt. Phys.* **1976**, *13*, 2287.
(7) Zhang, M.; Efremov, M. Y.; Schiettekatte, F.; Olson, E. A.; Kwan, A. T.; Lai, S. L.; Wisleder, T.; Greene, J. E.; Allen, L. H. *Phys. Rev. B: Condens. Matter Mater. Phys.* **2000**, *62*, 10548.
(8) Dick, K.; Dhanasekaran, T.; Zhang, Z. Y.; Meisel, D. *J. Am. Chem. Soc.* **2002**, *124*, 2312.
(9) Shibata, T.; Bunker, B. A.; Zhang, Z. Y.; Meisel, D.; Vardeman, C. F.; Gezelter, J. D. *J. Am. Chem. Soc.* **2002**, *124*, 11989.
(10) Sun, J.; He, L.; Lo, Y.-C.; Xu, T.; Bi, H.; Sun, L.; Zhang, Z.; Mao, S. X.; Li, J. *Nat. Mater.* **2014**, *13*, 1007.
(11) Xie, D.-G.; Wang, Z.-J.; Sun, J.; Li, J.; Ma, E.; Shan, Z.-W. *Nat. Mater.* **2015**, *14*, 899.
(12) Zhu, T.; Li, J. *Prog. Mater. Sci.* **2010**, *55*, 710.
(13) Tian, L.; Li, J.; Sun, J.; Ma, E.; Shan, Z.-W. *Sci. Rep.* **2013**, *3*, 2113.
(14) Plimpton, S. *J. Comput. Phys.* **1995**, *117*, 1.
(15) Zope, R.; Mishin, Y. *Phys. Rev. B: Condens. Matter Mater. Phys.* **2003**, *68*, 024102.
(16) Greer, J. R.; Oliver, W. C.; Nix, W. D. *Acta Mater.* **2005**, *53*, 1821.
(17) Zhu, T.; Li, J.; Samanta, A.; Leach, A.; Gall, K. *Phys. Rev. Lett.* **2008**, *100*, 25502.
(18) Sørensen, M. R.; Jacobsen, K. W.; Jóonsson, H. *Phys. Rev. Lett.* **1996**, *77*, 5067.
(19) Lu, Y.; Huang, J.; Wang, C.; Sun, S.; Lou, J. *Nat. Nanotechnol.* **2010**, *5*, 218.
(20) Wang, C.-C.; Mao, Y.-W.; Shan, Z.-W.; Dao, M.; Li, J.; Sun, J.; Ma, E.; Suresh, S. *Proc. Natl. Acad. Sci. U. S. A.* **2013**, *110*, 19725.
(21) Falk, M.; Langer, J. *Phys. Rev. E: Stat. Phys., Plasmas, Fluids, Relat. Interdiscip. Top.* **1998**, *57*, 7192.
(22) Li, W.; Rieser, J. M.; Liu, A. J.; Durian, D. J.; Li, J. *Phys. Rev. E* **2015**, *91*, 062212.
(23) Mei, Q.; Lu, K. *Prog. Mater. Sci.* **2007**, *52*, 1175.
(24) Gülseren, O.; Ercolessi, F.; Tosatti, E. *Phys. Rev. B: Condens. Matter Mater. Phys.* **1995**, *51*, 7377.
(25) Zhang, K.; Weertman, J.; Eastman, J. *Appl. Phys. Lett.* **2005**, *87*, 061921.
(26) MacGregor, C.; Fisher, J. *J. Appl. Mech.* **1945**, *12*, A217.
(27) Zener, C.; Hollomon, J. *J. Appl. Phys.* **1944**, *15*, 22.
(28) Medina, S., Hernandez, C. *Acta Mater.* **1996**, *44*.
(29) Strachan, D. R.; Smith, D. E.; Fischbein, M. D.; Johnston, D. E.; Guiton, B. S.; Drndic, M.; Bonnell, D. A.; Johnson, A. T. *Nano Lett.* **2006**, *6*, 441.
(30) Greenwood, J.; Williamson, J. *Proc. R. Soc. London, Ser. A* **1966**, *295*, 300.
(31) Persson, B. N. J. *Surf. Sci. Rep.* **2006**, *61*, 201.
(32) Akarapu, S.; Sharp, T.; Robbins, M. O. *Phys. Rev. Lett.* **2011**, *106*, 204301.
(33) Klajn, R.; Bishop, K. J.; Fialkowski, M.; Paszewski, M.; Campbell, C. J.; Gray, T. P.; Grzybowski, B. A. *Science* **2007**, *316*, 261.

DOI: 10.1021/acs.nanolett.5b02306
Nano Lett. 2015, 15, 6582−6585